Supplementary Materials for "Evaluation of Atmospheric Correction Algorithms over Lakes for High-Resolution Multispectral Imagery: Implications of Adjacency Effect"

S1. Waveband setting of the C-OPS

C-OPS A: 380, 395, 412, 443, 465, 490, 510, 532, 555, 560, 589, 625, 665, 683, 694, 710, 765, 780, 875 nm

C-OPS B: 320, 330, 340, 380, 412, 443, 465, 490, 510, 532, 555, 589, 625, 665, 683, 694, 710, 780, 875 nm

C-OPS C: 330, 380, 412, 443, 465, 490, 510, 532, 555, 565,589,625,665, 683, 694, 710, 765, 780, 875 nm

C-OPS D: 340,412, 443, 465, 490, 510, 532, 555, 560, 589, 625, 665,670, 683, 694, 710, 765, 780, 875 nm

S2. Main inputs of the 3D simulation

The main inputs of MCARATS are described as below:

1) Atmosphere profile

The NASA standard atmosphere profile of mid-latitude summer was used to calculate the extinction coefficient due to Rayleigh scattering, and the total gas absorption (see Figure S1).
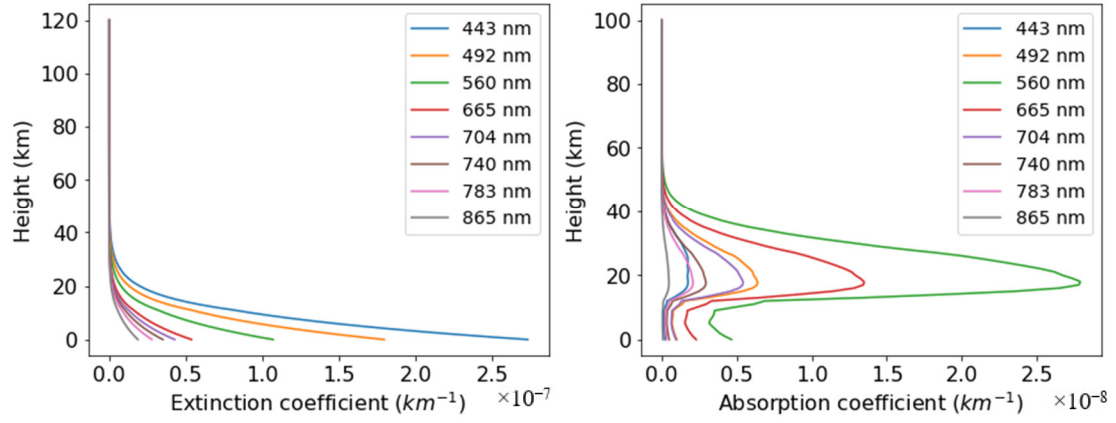
Figure S1. Extinction coefficient profile due to rayleigh scattering (left) and the total gas absorption coefficient profile (right).

2) Aerosol

An arbitrary vertical distribution of aerosol concentration was chosen to calculate the extinction coefficient profile due to aerosol scattering for a given AOT, Figure S2 illustrates the case of AOT=0.06 (see Figure S2). The aerosol type and the AOT for the simulation for the ideal and real case are described below.
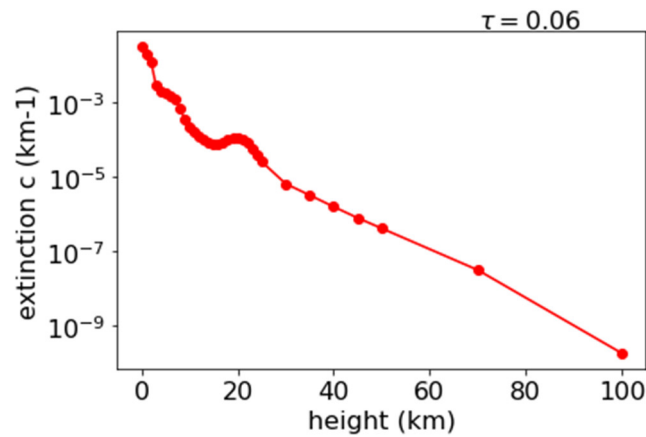
Figure S2. The extinction coefficient profile due to aerosol scattering with AOT=0.06.

- Ideal case

An arbitrary aerosol type with relative humidity of 70 and fine-mode fraction of 0 from the Ahmad2010 model, and a moderate aerosol concentration (AOT(865)=0.1) was used as the inputs of aerosol.

- Real case

The SEN2COR-derived AOT at 550 nm (0.065) was used as the reference, AOT at other bands of S2/MSI were calculated based on the aerosol type adopted in SeaDAS. Since the aerosol type or *angstrom* coefficients were not available in the SEN2COR level-2 product, we tested different aerosol types in the SeaDAS aerosol model, the one that made the minimum difference between the simulation and observation was chosen as the optima. In this study the optimal aerosol type is the one with relative humidity of 70 ,and fine mode index of 95.
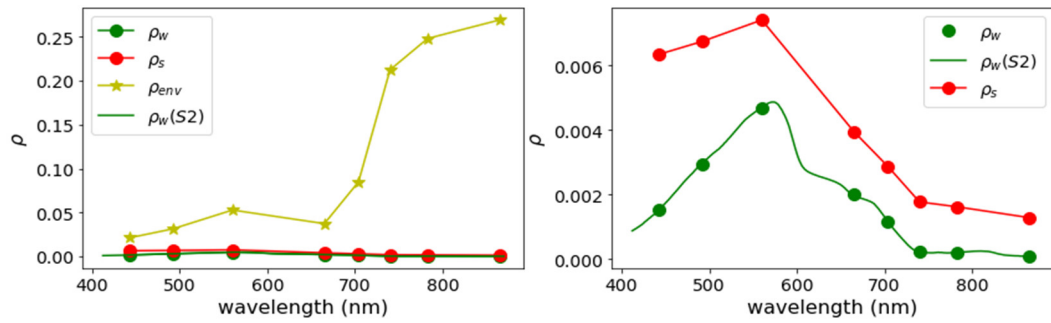
3) Surface reflectance.

- Ideal case

The surface reflectance of the water body and the environment (green vegetation) are shown in Figure S3. The surface reflectance of the environment was arbitrarily taken from a green vegetation region in google earth engine.
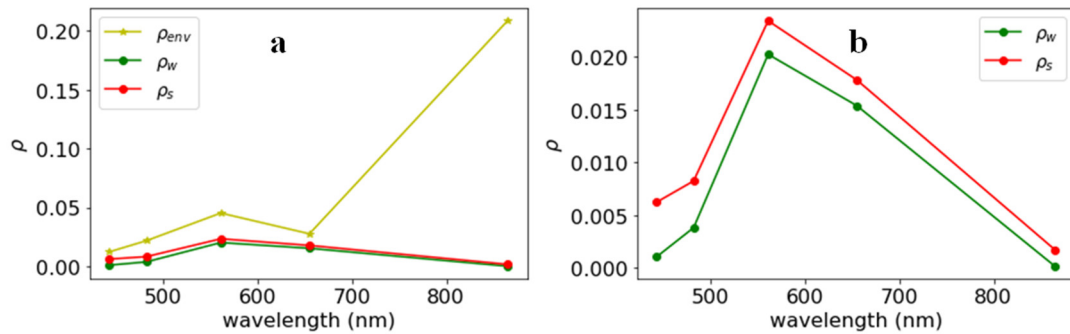
Figure S3. Surface reflectance in the L8/OLI VNIR bands for the simulation. (a) Surface reflectance of the water body ρ_s (read) including the reflected diffuse skylight, and the environment (ρ_{env}, yellow), (b) Zoom plot of the Surface reflectance spectrum of the water body. The reflectance due to the water-leaving radiance ρ_w is also shown as a green line.

● Real case

The SEN2COR-derived bottom reflectance from the S2/MSI image (S2B_MSIL1C_20190829T190919_N0208_R056_T10UED_20190829T21) was used for the land surface reflectance, but the water reflectance was replaced by the in situ measurement. Figure S4 illustrates the reflectance of the water body and the averaged reflectance of environment.


Figure S4. Surface reflectance in the S2/MSI VNIR bands for the simulation. (a) Surface reflectance of the water body ρ_s (read) including the reflected diffuse skylight, and the averaged reflectance of the environment (ρ_{env}, yellow), (b) Zoom plot of the Surface reflectance spectrum of the water body. The reflectance due to the water-leaving radiance ρ_w is also shown as a green line.

4) Observation geometry

For the real case, the solar zenith, viewing zenith, and relative azimuth were taken from the SEN2COR level 2 product, which was 44.9, 8.0, 118 degrees; for the ideal case, the solar zenith, viewing zenith were set as 30, 0 degrees.
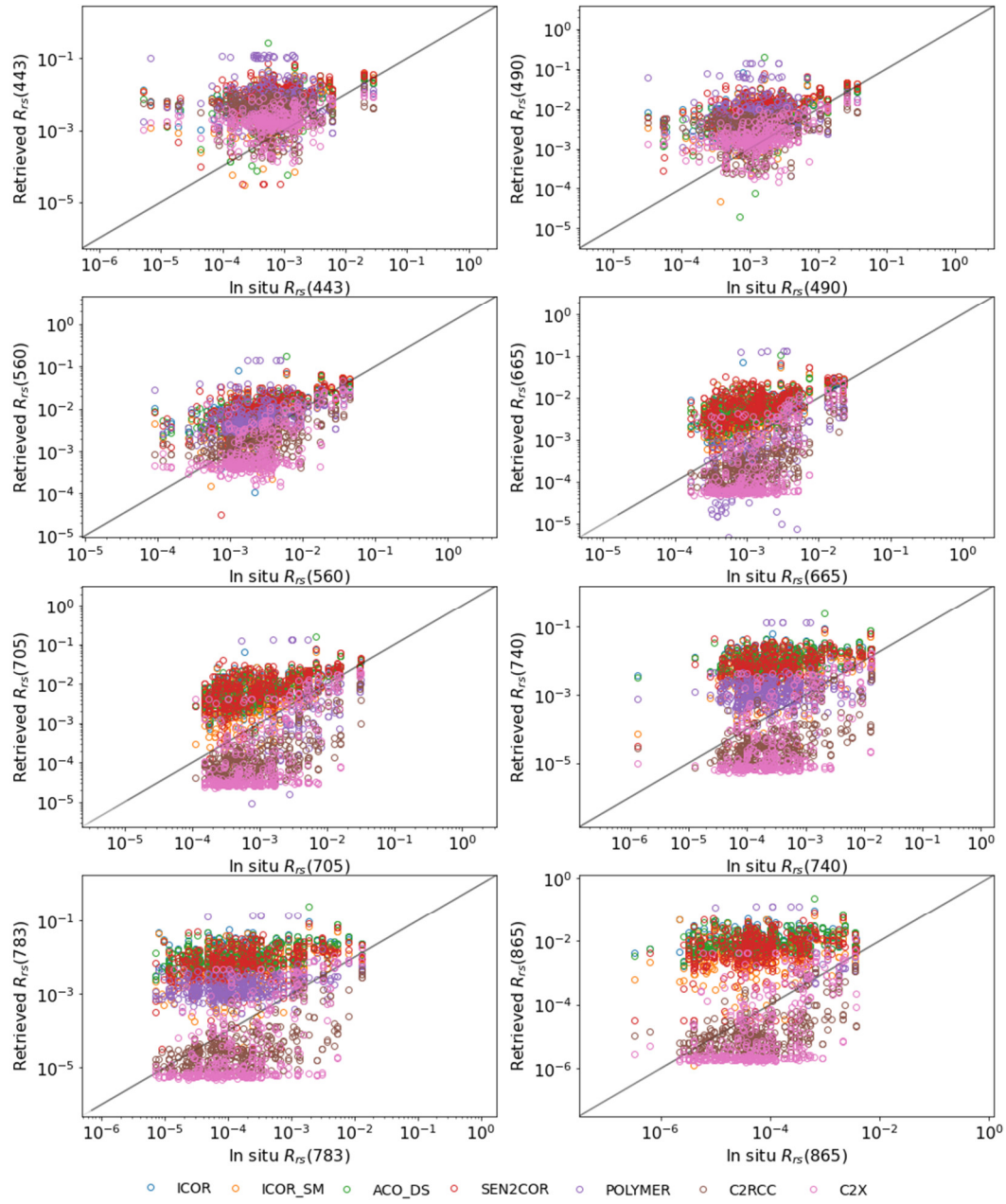
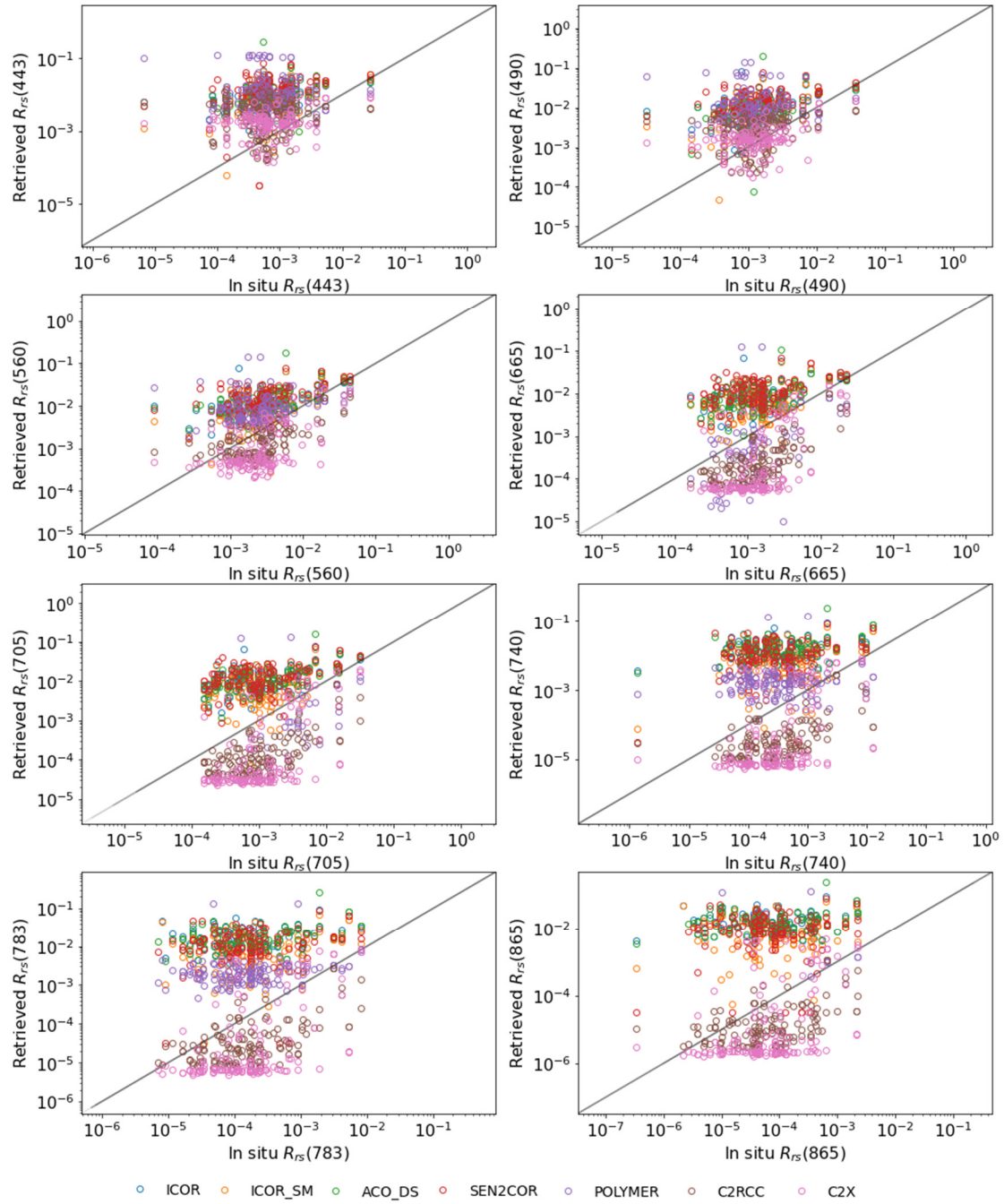**S3. Scatter plots of the validation**
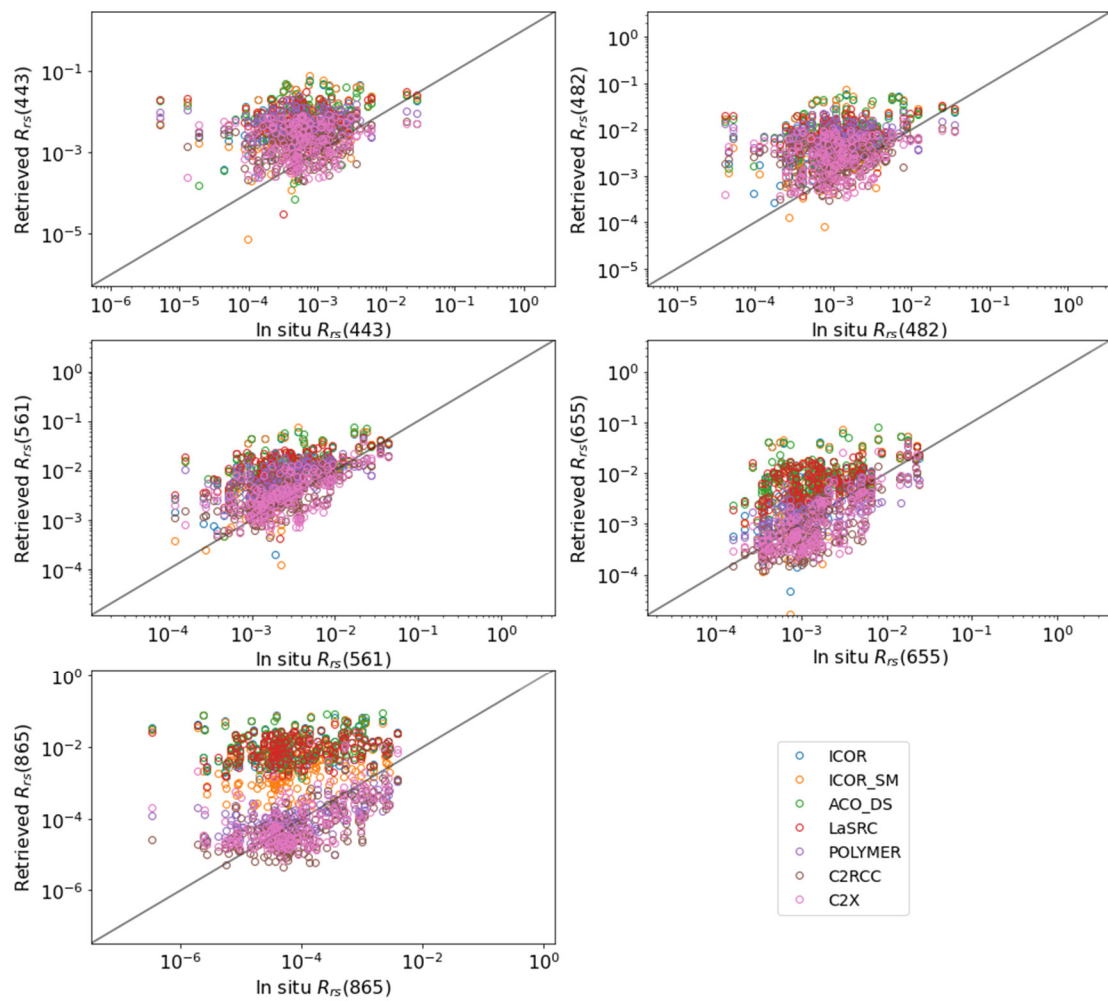
Figure S5. Scatter plots of the *in situ* measured R_{rs} and the R_{rs} retrieved by different algorithms in Landsat-8 OLI bands for the G-ALL group.
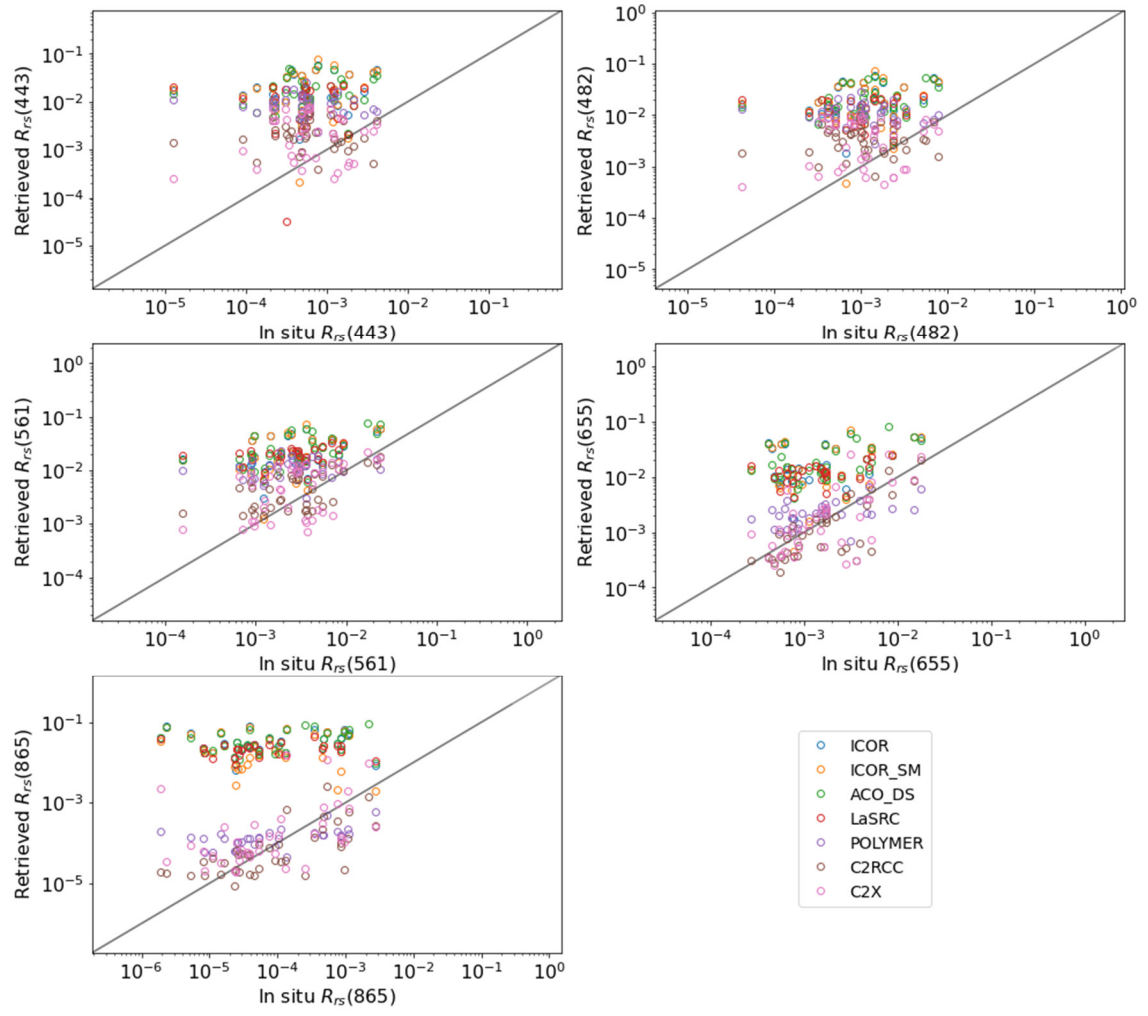
Figure S6. Scatter plots of the *in situ* measured R_{rs} and the R_{rs} retrieved by different algorithms in Landsat-8 OLI bands for the G-CIRRUS group.
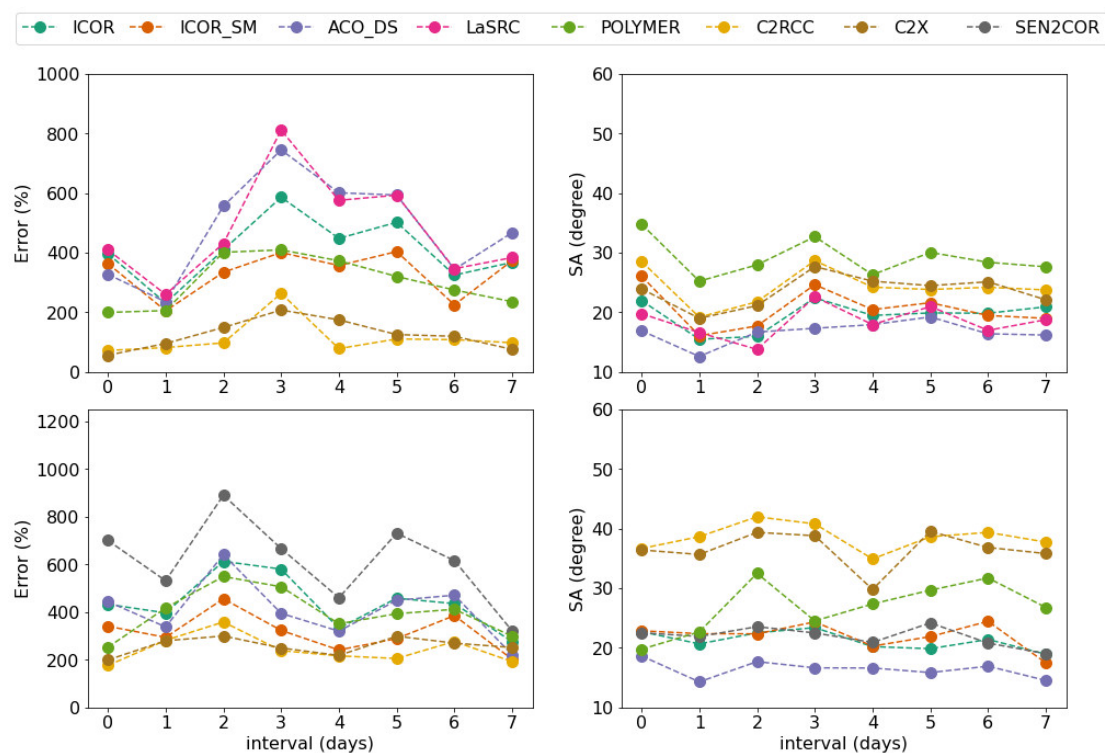
Figure S7. Scatter plots of the *in situ* measured R_{rs} and the R_{rs} retrieved by different algorithms in Sentinel-2 MSI bands for the G-ALL group.

Figure S8. Scatter plots of the *in situ* measured R_{rs} and the R_{rs} retrieved by different algorithms in Sentinel-2 MSI bands for the G-CIRRUS group.

S4. Discussion

Figure S9. Error and SA for matchups with different intervals for Landsat-8 OLI (upper) and Sentinel-2 MSI (bottom).